

should be greater than 10^{-19} cm².

(b) **Rate of Decrease of $\sigma_{\text{net}}(E)$.** Although C₆F₆ has actually a smaller cross section than SiF₄ (Table I) it absorbs almost twice as much energy at the same fluence (Table II). This is attributable to the fact that $\sigma_{\text{net}}(E)$ decreases with energy more slowly in the case of C₆F₆ (Figure 5). If n vs. F curves for the two molecules are constructed, that for C₆F₆ shows smaller departure from linearity indicating $\sigma^{\text{expl}}(F) \approx \text{constant}$. In this sense it behaves as a pseudo-Lambert-Beer absorber.

(c) **Heat Capacity.** At reasonably high pressures (e.g., in sensitized systems) where thermalization competes with excitation it has proven useful to consider the system as having acquired an effective temperature (T_{eff})^{6,33} at which reaction may occur. In this respect the amount of energy absorbed must be considered in conjunction with the heat capacity of the system. T_{eff} is defined through the equation $E_{\text{abs}} = \int_{298}^{T_{\text{eff}}} C_v dT$ where E_{abs} is the absorbed energy and C_v is the heat capacity of the system. As an example, compare SiF₄ and C₆F₆ (Table II). C₆F₆ absorbs more energy than SiF₄, yet it reaches a T_{eff} of only ~ 1350 K while SiF₄ reaches a T_{eff} of ~ 2050 K. This difference stems from the larger heat capacity of C₆F₆. On the other hand for the molecules SiF₄ and C₄H₆O which have rather similar heat capacities, values of T_{eff} are seen to follow the relative amounts of energy absorbed. Most marked is the case of C₆F₆ and NH₃ which have similar T_{eff} although C₆F₆ absorbs almost seven times as much energy. These effects can all be traced to the difference in C_v of the pairs compared.

6. Absorption Laws for Different Pulse Lengths and Higher Fluences. Equation 1 is a convenient way of summarizing the experimental data. Although it is often assumed that the temporal evolution is fluence rather than intensity dependent,²⁶ recent experimental data cast doubt on the generality of this.⁵ This means

(33) Burak, I.; Quelly, T. J.; Steinfeld, J. I. *J. Chem. Phys.* **1979**, *70*, 334.

(34) Herzberg, G. "Molecular Spectra and Molecular Structure"; Van Nostrand: Princeton, N.J., 1960; Vol. II.

(35) Clark, R. J. H.; Rippon, D. M. *J. Mol. Spectrosc.* **1972**, *44*, 479.

(36) Stigliani, W. M.; Laurie, V. W.; Scharpen, L. H. *J. Mol. Spectrosc.* **1976**, *62*, 85.

that the values of the A_1 , A_2 , B_1 , etc., parameters may be dependent on the nature of the pulse, in particular pulse length (as well as upon pressure). Under these circumstances, provided $\sigma_{\text{net}}(E)$ still decreases with increasing E , we in general have $\sigma^{\text{expl}}(F) \lesssim d \int_{E_T}^{\infty} \sigma_{\text{net}}(E) p(E) dE$.

Also notice that although at moderate fluences $\bar{n} \propto F^m$ with $m < 1$ (see Figure 9), at the highest fluences the exponent of fluence reverts to unity in eq 1. However, most evidence indicates that at very high powers $m < 1$. Indeed recent measurements on SiF₄ at high fluences (>2 J/cm²)³² have shown that eq 1 predicts values of n higher than those actually observed. This suggests that the term $A_2 F^2$ in eq 1 should be replaced by $A_2' F^{(1+x)}$ where $x < 1$ and is probably close to $2/3$.^{4b}

Conclusions and Summary

For fluences ~ 1 J/cm² experimental data can be conveniently summarized in terms of parameters A_1 , A_2 , and B_1 associated with an empirical differential absorption law (eq 1). The data can also be conveniently expressed in terms of $\sigma^{\text{expl}}(F)$. This differential cross section at fluence F can in turn be related, through a simple model for multiple photon excitation, to the net microscopic cross section associated with the "energy shell" of energy E . In the limit of low fluence, $\sigma^{\text{expl}}(F)$ becomes the low-signal absorption cross section σ_0^{expl} .

All molecules studied have $\sigma_{\text{net}}(E)$ decreasing with increasing E . The factors influencing this dependence include anharmonicity as well as molecular complexity.

In laser chemistry the nature and extent of reaction depend strongly upon E_{abs} and, under conditions in which molecules can be regarded as reaching an effective temperature, upon T_{eff} . The efficiency with which molecules harvest energy from the laser field will depend not only upon σ_0^{expl} but also upon the rate of decrease of $\sigma_{\text{net}}(E)$. In addition T_{eff} will also reflect the effective heat capacity of the system.

Acknowledgment. We thank Dow Chemical Corporation and NIH through a Biomedical Support Grant to Brandeis University for financial support.

Infrared Multiphoton Absorption by Medium-Sized Molecules in the Gas Phase. Hexafluorobenzene and 2,3-Dihydropyran[†]

Michael T. Daignan, Dana Garcia, and Ernest Grunwald*

Contribution from the Department of Chemistry, Brandeis University, Waltham, Massachusetts 02254. Received April 2, 1981.

Revised Manuscript Received September 17, 1981

Abstract: Multiphoton IR absorption by C₆F₆ at 1023 cm⁻¹ and by C₃H₈O at 1072 cm⁻¹ was found to be independent of pressure and square-pulse equivalent (SPE) pulse width under the following conditions. For C₆F₆: P , 0.257–10.1 torr; SPE width, 80–330 ns; fluence, 0–0.7 J cm⁻²; E_{abs} , 0–300 kJ/mol. For C₃H₈O: P , 11–36 torr; SPE width, 0.37–1.45 μ s; fluence, 0–1.0 J cm⁻²; E_{abs} , 0–130 kJ/mol. It is argued that the relative simplicity of these absorption laws, especially for C₆F₆, is related to physical properties generally shared by medium-sized and large molecules. A model is presented which reproduces the data for the present substrates with just one specific parameter. Results are also reported for IR absorption by SiF₄-C₃H₈O mixtures.

Basic knowledge of multiphoton absorption from high-power infrared laser sources is important to the control and interpretation of IR laser photochemistry. For small molecules an impressive amount of information is available, and convenient systematics for describing multiphoton absorption has been developed.²⁻⁵ The phenomenology for small molecules is complicated. Absorption cross sections depend not only on temperature (or specific vi-

brational excitation) but also on pressure, intensity, and IR pulse shape.²⁻⁵

(1) Grateful acknowledgment is made to grants in support of parts of this work by the National Science Foundation and the Edith C. Blum Foundation.

(2) (a) Starov, V.; Steel, C.; Harrison, R. G. *J. Chem. Phys.* **1979**, *71*, 3304. (b) Starov, V.; Selamoglu, N.; Steel, C. *J. Phys. Chem.* **1981**, *85*, 320.

(3) (a) Judd, O. P. *J. Chem. Phys.* **1979**, *71*, 4515. (b) Quigley, G. P. *Springer Ser. Chem. Phys.* **1978**, *3*, 374.

(4) Baldwin, A. C.; Barker, J. R. *J. Chem. Phys.* **1981**, *74*, 3823.

[†] Dedicated to George S. Hammond on the occasion of this 60th birthday.

In this paper we report multiphoton IR absorption results for two medium-sized molecules, hexafluorobenzene (C_6F_6) and 2,3-dihydropyran (C_5H_8O). These molecules have 30 and 36 vibrational modes, respectively, and vibrational state densities are considerable even at room temperature. We find that for both substances, absorption cross sections are simple functions of absorbed energy, being virtually independent of pressure and IR pulse shape under all experimental conditions.

Notation and Definitions. As much as possible, notation follows that used in the preceding paper:⁵ I = instantaneous intensity at time t ($W\ cm^{-2}$); $F(t) = \int_0^t I(t')\ dt'$, fluence ($J\ cm^{-2}$) delivered in the time interval 0 to t ; F_p = fluence due to the full laser pulse; $E_a(t)$ = energy absorbed (J/mol) in the time interval 0 to t ; and E_{abs} = energy absorbed (J/mol) from the full laser pulse—all measured in a given small element of volume.

Instantaneous ensemble averages of molecular properties are denoted by bar superscripts. Partial averages of molecular properties (for specified subsets of the molecules) are denoted by circumflex superscripts. For example, $\bar{\sigma}(t_1)$ denotes the average absorption cross section per molecule at time t_1 , and $\bar{\sigma}(E_v)$ at t_1 denotes the average absorption cross section per molecule in a narrow molar vibration energy range δE_v centered on E_v .

Optical cells used in the present work are "thin" so that, except for a brief analysis in the Experimental Section, the "optical depth problem" described by Starov et al.⁵ has been avoided.

Our experiments determine E_{abs} as functions of F_p and thus define an average cross section (σ^{exptl} , $cm^2/molecule$) for absorption from the full laser pulse (eq 1), where N_0 = Avogadro's number.

$$N_0\sigma^{exptl} = E_{abs}/F_p \quad (1)$$

However, the instantaneous cross section ($\bar{\sigma}$) may vary with $E_a(t)$ and thus is defined in terms of the rate of absorption; at time t_1 during the laser pulse $\bar{\sigma}(t_1)$ is given by (2). Integration of (2)

$$N_0\bar{\sigma}(t_1) = \Gamma^{-1}(dE_a/dt)_{t_1} = (dE_a/dF)_{t_1} \quad (2)$$

over the full pulse and substitution in (1) yields (3), which shows that σ^{exptl} is a fluence-average of $\bar{\sigma}$.

$$\sigma^{exptl} = \int_{\text{pulse}} \bar{\sigma}\ dF/F_p \quad (3)$$

The small-signal (i.e., low-intensity) cross section $\bar{\sigma}_0$ is the limit reached by $\bar{\sigma}$ as the incident intensity goes to zero. For medium-sized molecules the rotational fine structure of vibrational absorption bands⁶ is dense enough to merge into a quasi-continuum, so that Beer's law holds at low intensities and $-\ln I/dl = kC$, where C = absorber concentration ($mol\ cm^{-3}$), l = optical path length (cm), and k is the formal extinction coefficient at the given wavenumber $\bar{\nu}$. ($k/2303$ is the conventional decadic molar extinction coefficient.) It can be shown, by considering thin cells, that $N_0\bar{\sigma}_0 = k$.

Experimental Section

Materials. Hexafluorobenzene (Aldrich) and 2,3-dihydropyran (Aldrich, redistilled) were further purified by out gassing and were found by GC mass spectral or GC analysis to be >99.9% and >99% pure, respectively. Silicon tetrafluoride gas (Matheson, 99.6%) was used without further purification.

Infrared Calorimetry. The amounts of infrared energy absorbed by the gaseous samples were measured by disk calorimetry, as described earlier.⁷ Absolute accuracy of transmitted IR energy was 3% or better; accuracy of absorbed energy was 10% or better. The principal instrumental improvement was the use of a polarizer-attenuator (II-VI Corp.) in place of CaF_2 flats in the C_6F_6 measurements. A 2:1 beam concentrator (II-VI Corp.) was used in a few experiments to boost intensity in short pulses.

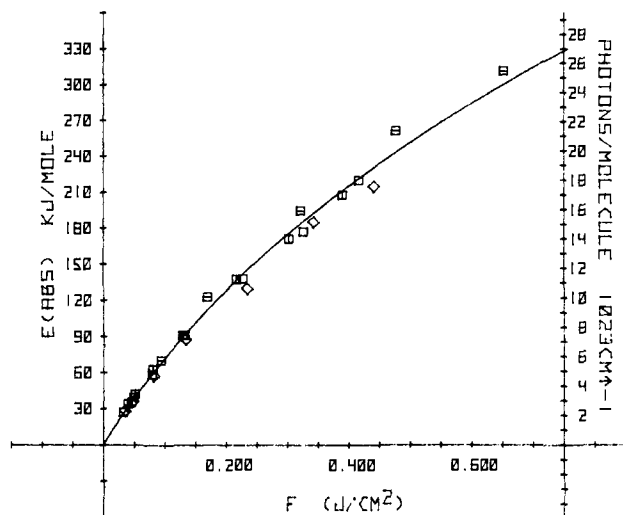


Figure 1. IR absorption by C_6F_6 at $1023\ cm^{-1}$ as a function of F_p and P : open squares, 0.257 torr; vertical shading, 1.32 torr; horizontal shading, 1.77 torr; diamonds, 7.10 torr (SPE width = 330 ns). The smooth curve is based on (23). Parameters $\bar{\sigma}(0)$ and β are given in the text.

IR Pulse Profiles. Multimode IR laser pulses from a Lumonics Model 103 CO_2 laser were used in all experiments. Intensity profiles of the CO_2 laser pulses were measured with a Rofin Model 7410 photon drag detector and displayed on a Tektronix Model 7633 storage oscilloscope; a second photon drag detector provided the time-base trigger voltage.⁷ In testing the dependence of IR absorption on pulse-intensity profile, the latter was changed either by changing the relative concentration of N_2 in the CO_2 laser cavity or by pulse truncation after 100 or 200 ns with a plasma shutter built especially for that purpose. Mode beats were observed in each pulse-intensity profile, but the beat patterns were not highly reproducible, suggesting radiation coherence times of the order of 10 ns. Typical profiles for untruncated pulses have been reported.^{7,8,14}

Plasma Shutter.⁸ A plasma shutter⁹ was used to truncate the microsecond-long tail characteristic of CO_2 TEA lasers. The principle of operation centers on the initiation of a plasma avalanche which creates an overdense plasma, blocking further transmission of the IR beam. The shutter should be electronically triggered at an adjustable time after the start of the IR pulse. Its design is similar in principle to one already reported in the literature.¹⁰ Briefly, it consisted of a 1:1 telescope constructed from 2.5-cm diameter, 3.8-cm focal length germanium meniscus-type lenses. The focal area was bathed in liquid- N_2 boil-off vapors to prevent premature avalanche seeding on dust particles. A positionable spark gap constructed from tungsten electrodes was placed at the focal point perpendicular to the beam. A photon drag detector sensed the start of the IR pulse and, after a suitable delay, triggered a fast high-voltage pulser. The pulser in turn fired the spark gap, thereby initiating the plasma avalanche. Delays were selected to give 100- and 200-ns pulse widths (SPE's, 80 and 165 ns; see eq 7). When it was desired to compare the effects of truncated and nontruncated pulses, the high-voltage pulser was merely switched off and no shuttering occurred, all other variables being held constant.

Optically Thin Cells. It has been stressed by Starov et al.⁵ that measurements of σ^{exptl} must involve optically thin cells. We now wish to summarize an analysis which shows that cells may be regarded as optically thin even if as much as 40% of the incident fluence is absorbed.

Adopting the notation of ref 5, Figure 1: let F_0 and F_l denote fluence at front and rear window, respectively, inside the cell. Let $F_{abs} = F_0 - F_l$ and $F_p = (F_0 + F_l)/2$. Let l denote distance from front window along the optical path inside the cell. Let $l = L$ at the rear window and $l = l_p$ at the point where $F = F_p$. The precise value of l_p/L will depend on the absorption law for the given sample.

Using the absorption laws actually found for C_6F_6 and C_5H_8O (Figures 1-3), we have compared F_{abs}/L with $-dF/dl$ at l_p . The comparison is relevant because when $F = F_p$, $N_0\sigma^{exptl} = -C^{-1}F_p^{-2}(dF/dl)$ at l_p , by

(5) Starov, V.; Selamoglu, N.; Steel, C. *J. Am. Chem. Soc.*, preceding article in this issue.

(6) Wilson, E. B.; Decius, J. C.; Cross, P. C. "Molecular Vibrations"; Dover Publications: New York, reprinted 1980; pp 162-166, 193-196.

(7) (a) Grunwald, E.; Olszyna, K. J.; Dever, D. F.; Knishkowsky, B. *J. Am. Chem. Soc.* 1977, 99, 6515. (b) Garcia, D.; Grunwald, E. *Ibid.* 1980, 102, 6407.

(8) Duignan, M. T. Ph.D. Thesis, Brandeis University, 1981, may be consulted for further details.

(9) (a) Yablonovitch, E. "Laser Interactions and Related Plasma Phenomena"; Plenum Press: New York, 1977; Vol. 4A. (b) Yablonovitch, E. *Phys. Rev. A* 1974, 10, 1888.

(10) Kwok, H. S.; Yablonovitch, E. *Rev. Sci. Instrum.* 1975, 46, 814; *Appl. Phys. Lett.* 1975, 27, 583.

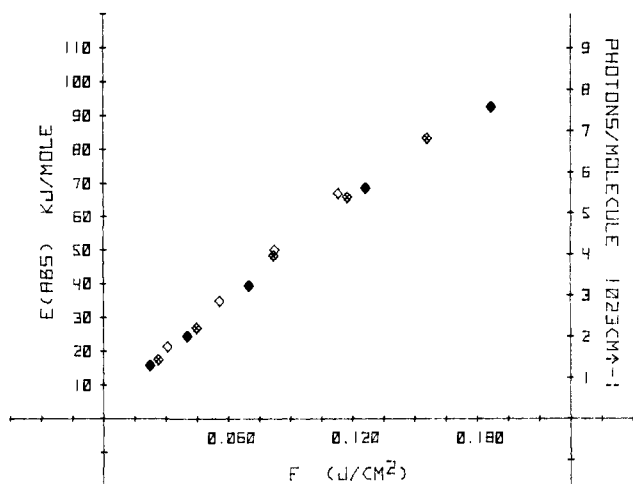


Figure 2. IR absorption by C_6F_6 at 1023 cm^{-1} as a function of intensity ($P = 4.73\text{ torr}$). SPE width: open diamonds, 80 ns; shaded diamonds, 165 ns; solid diamonds, 330 ns.

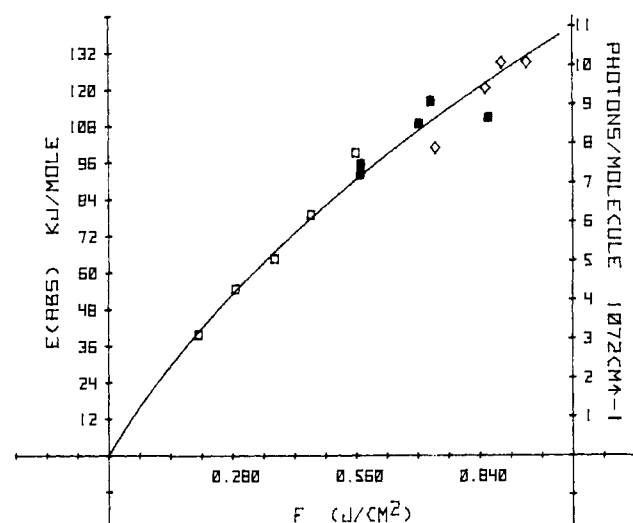


Figure 3. IR absorption by C_6H_8O at 1072 cm^{-1} as a function of F_p and I_p . Sample pressures range from 11 to 36 torr. SPE width: open squares, 370 ns; solid squares, 680 ns; diamonds, 1.45 μs . The smooth curve is based on (22b), assuming fast $V-T/R$ relaxation. Parameters $\bar{\sigma}(0)$ and β are given in the text.

definition.⁵ For a "thin" cell ($L \rightarrow 0$), $F_{\text{abs}}/L = -dF/dl$ at I_p .

As L increases, these quantities diverge. However, our analysis shows that their ratio is given by (4). In (4), $\varphi(F_p)$ is a function of F_p whose

$$-\frac{F_{\text{abs}}}{L} \left/ \left(\frac{dF}{dl} \right)_{I_p} \right. = 1 - \frac{1}{12} \left(\frac{F_{\text{abs}}}{F_p} \right)^2 \varphi(F_p) + O\left(\frac{F_{\text{abs}}}{F_p} \right)^4 \quad (4)$$

value is always near unity and whose upper bound (as F_p becomes large) is 2. $O(F_{\text{abs}}/F_p)^4$ denotes a term $\lesssim (F_{\text{abs}}/F_p)^4$.

According to (4), cells are "thin" within 2% if $F_{\text{abs}}/F_p < [0.24/\varphi(F_p)]^{1/2}$. Since $\varphi(F_p) \approx 1$, F_{abs}/F_p must be $\lesssim 0.5$. That is, cells are "thin" within 2% if $\lesssim 40\%$ of the incident fluence is absorbed. The present experiments satisfy that criterion.

Results

Hexafluorobenzene. Because of its high thermal stability, IR absorption by C_6F_6 can be studied up to absorbed energies (E_{abs}) of at least 300 kJ/mol without significant decomposition. When thermal reaction does occur,^{8,11-13} the chief gaseous product (C_2F_4) and some lesser products ($CF_3C_6F_5$, C_3F_6 , C_4F_8) suggest that CF_2 is a reaction intermediate. There is also an amorphous solid

Table I. Effect of Pressure on IR Absorption by 2,3-Dihydropyran at 1072 cm^{-1}

F_p , J/cm ² (t_{SPE} , μs)	P , torr	$10^{-5} E_{\text{abs}}/F_p$, cm ² /mol ⁻¹
0.204 (0.37)	15.0	1.94
	24.2	1.97
	31.7	1.95
0.705 (0.68)	15.2	1.58
	19.6	1.55
	28.7	1.35
	36.0	1.60
0.952 (1.45)	11.3	1.40
	14.9	1.33
	25.2	1.32
	30.4	1.30

residue, as well as traces of CF_4 and C_2F_6 .

Figure 1 shows results obtained for absorption at 1023 cm^{-1} (CO_2 laser line P44) as a function of fluence at C_6F_6 pressures of 0.25–7.1 torr. These measurements involved pulses with a constant intensity–time profile and variable attenuation; their square-pulse equivalent width was 330 ns (see below). Within the experimental error all data points follow a single relationship; i.e., $E_{\text{abs}}(F_p)$ is independent of pressure. This same relationship is also consistent with data obtained in optically thick cells at 20–48 torr.¹⁴

Figure 2 shows results obtained for $E_{\text{abs}}(F_p)$ at a constant pressure of 4.73 torr. Beam intensity was varied by truncating the pulses used in obtaining Figure 1 with a plasma shutter after 100 and 200 ns, respectively.

Before Figure 2 is interpreted, some explanation may be in order. The intensity profiles of multimode CO_2 laser pulses are highly complicated functions of time. Fortunately, much of this complexity is irrelevant to the description of E_{abs} . If the absorption cross section $\bar{\sigma}$ is independent of intensity I , one needs only the fluence $F_p = \int I dt$ for the given pulse. If $\bar{\sigma}$ is a linear function of I , one needs both F_p and the mean intensity I_p at which the fluence is delivered, as defined in (5). Experiment yields the pulse

$$I_p = F_p^{-1} \int I dt \quad (5)$$

profile $I(t)$. I_p may then be derived by (6) for the given pulse.

$$I_p = \int I^2 dt / \int I dt \quad (6)$$

The square-pulse equivalent (SPE) width for the given intensity profile is defined in (7). When $\bar{\sigma}$ is a nonlinear function of I ,

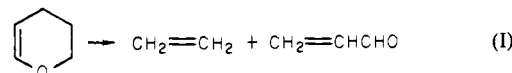
$$t_{\text{SPE}} = F_p/I_p = \left(\int I dt \right)^2 / \int I^2 dt \quad (7)$$

one needs F_p and I_p , as well as higher power integrals. However, to test merely whether $\bar{\sigma}$ is independent of I , it is sufficient to measure $E_{\text{abs}}(F_p)$ for a range of values of t_{SPE} .

For the data plotted in Figure 2, t_{SPE} is 80, 165, and 330 ns, respectively. Within the experimental error, $E_{\text{abs}}(F_p)$ is independent of t_{SPE} . We conclude that in this series, $\bar{\sigma}$ is independent of I .

Similar experiments are available at 10.1 and 1.35–1.55 torr.⁸ These experiments all seem to define a single relationship $E_{\text{abs}}(F_p)$, independent of I_p . Deviations of >10% from the average relationship were obtained in only two experiments, both at 1.55 torr, where the deviations were within 20%. We do not believe they are physically real.

2,3-Dihydropyran. On IR excitation this substrate undergoes the retro-Diels–Alder reaction (I)^{7b,15} and the half-chair-to-boat



conformational equilibrium shifts toward the boat form.^{7b}

(11) Desirant, Y. *Bull. Soc. Chim. Belg.* **1958**, *67*, 676.

(12) Gilbert, R.; Theoret, A. *J. Phys. Chem.* **1976**, *80*, 1017.

(13) Petrova, T. D.; Platonov, V. E.; Gorfinkel, M. I.; Yakobson, G. G. *Zh. Org. Khim.* **1975**, *11*, 2123.

(14) Spelser, S.; Grunwald, E. *Chem. Phys. Lett.* **1980**, *73*, 438.

(15) Garcia, D.; Keehn, P. M. *J. Am. Chem. Soc.* **1978**, *100*, 6111.

However, unless $E_{\text{abs}} \geq 150$ kJ/mol, (I) is too slow to be significant during the very short time in which IR absorption occurs^{7b} (>99.9% of the fluence is delivered in less than 3 μ s). In the present experiments, E_{abs} ranged up to 130 kJ/mol.

On the other hand, half-chair-to-boat equilibration lags behind IR absorption by <50 ns.^{7b} However, calculations using the known equilibrium constant led to the conclusion that the effect of this process on σ^{exptl} is inconsiderable.

Table I shows results of E_{abs} as a function of P at 1072 cm^{-1} (CO_2 laser line R10) under various conditions of IR fluence and pulse shape. Within the experimental range (11–36 torr) the data show no significant pressure dependence.

Figure 3 shows the concordance of E_{abs} vs. F_p for data obtained with different pulse shapes and t_{SPE} . It appears that σ^{exptl} is independent of I . This conclusion is strongly reinforced by the finding, reported earlier,^{7b} that the absorption coefficient during a single pulse remains constant (with 9% standard deviation) over a 50-fold variation of intensity.

$\text{SiF}_4 + \text{C}_5\text{H}_8\text{O}$. In connection with SiF_4 -sensitized IR-photoinduced reactions of 2,3-dihydropyran,¹⁶ binary gas mixtures were irradiated at 1025.3 and 1031.5 cm^{-1} (CO_2 laser lines P42 and P36). This is in the region of the very strong 1032- cm^{-1} degenerate stretching band of SiF_4 . Accurate results were obtained for IR absorption. These are worth reporting because the phenomenology was unexpectedly simple.

For SiF_4 , low-intensity cross sections $\bar{\sigma}_0$, measured by IR spectrophotometry, are 3.4×10^{-18} cm^2 at 1025 cm^{-1} and $\sim 7 \times 10^{-18}$ cm^2 at 1032 cm^{-1} . $\text{C}_5\text{H}_8\text{O}$ absorbs only weakly: $\sigma_0 \approx 0.03 \times 10^{-18}$ cm^2 at 1032 cm^{-1} and practically no absorption at 1025 cm^{-1} .

With the assumption of only additive contributions, E_{abs} per mole of binary mixture is given by (8), where X_1 and X_2 denotes

$$E_{\text{abs}}/F_p = N_0(\sigma_1^{\text{exptl}}X_1 + \sigma_2^{\text{exptl}}X_2) \quad (8)$$

mole fraction. In 12 experiments at 1025.3 cm^{-1} , F_p ranged from 0.2 to 0.9 J cm^{-2} , P_{SiF_4} from 3.6 to 18 torr, X_{SiF_4} from 0.12 to 0.27, and total pressure from 29 to 69 torr. Absorption was essentially independent of $X_{\text{C}_5\text{H}_8\text{O}}$. $E_{\text{abs}}/(F_p X_{\text{SiF}_4})$ was $(9.8 \pm 0.8) \times 10^5$ $\text{cm}^2 \text{mol}^{-1}$ and σ^{exptl} for SiF_4 was accordingly 1.6×10^{-18} cm^2 . In the absence of $\text{C}_5\text{H}_8\text{O}$, σ^{exptl} for SiF_4 is a strong function of F_p and P_{SiF_4} .⁵

In seven experiments at 1031.5 cm^{-1} , F_p ranged from 0.65 to 0.9 J cm^{-2} , P_{SiF_4} from 9 to 23 torr, X_{SiF_4} from 0.21 to 0.57, and total pressure from 34 to 60 torr. $E_{\text{abs}}/(F_p X_{\text{SiF}_4})$ ranged from 5.34×10^5 to 2.71×10^5 $\text{cm}^2 \text{mol}^{-1}$ and was essentially linear in mole fraction, indicating constant cross sections σ^{exptl} in (8). The standard error of the linear fit according to (8) was 5%: $\sigma^{\text{exptl}} = 0.55 \times 10^{-18}$ cm^2 for SiF_4 and 0.12×10^{-18} cm^2 for $\text{C}_5\text{H}_8\text{O}$.

Discussion

Compared to multiphoton absorption by small molecules such as NH_3 ,^{2a} SF_6 ,⁴ and SiF_4 ,⁵ absorption laws obtained for C_6F_6 and $\text{C}_5\text{H}_8\text{O}$ are simple. In particular for C_6F_6 , E_{abs} at constant F_p is practically independent of pressure and I_p over substantial ranges. Results for $\text{C}_5\text{H}_8\text{O}$, though limited to relatively high pressures (>10 torr), are in a pressure range in which $E_{\text{abs}}(F_p)$ for NH_3 and SiF_4 depend significantly on P .

Pressure and IR saturation effects will of course disappear in the high-pressure limit when collisional redistribution of energy and attainment of thermal equilibrium become fast compared to IR absorption. It is of interest whether this may have happened in our experiments.

When a collision diameter of 6.97 Å is adopted for C_6F_6 ,¹⁷ the mean time between gas-kinetic collisions at 298 K is $78/(P/\text{torr})$ ns per molecule and thus ranges in the present experiments from 304 ns at 0.257 torr to 7.7 ns at 10.1 torr for C_6F_6 . The effective IR pulse width t_{SPE} ranges from 80 to 330 ns. Overall, the ex-

periments span a range of ~ 1 –40 collisions per molecule during the IR pulse in which, when $F_p = 0.4$ J/cm^2 , a mean of 18 IR photons is absorbed.

At the lower pressures (ca. 1 collision per molecule per pulse), IR absorption by C_6F_6 thus takes place mostly under collisionless conditions. The developing energy distribution probably resembles that in a model described recently by Baldwin and Barker.⁴ That is, there will be population peaks in discrete, fairly narrow energy bands corresponding to absorption of 1, 2, 3, IR photons by molecules of the initial room-temperature distribution.

At the higher C_6F_6 pressures (~ 40 collisions per molecule per pulse) these population peaks will be largely eroded by collisions. It seems likely, therefore, that the experiments with C_6F_6 cover a substantial range of absorbing molecular energy distributions.

By contrast, similar calculations for $\text{C}_5\text{H}_8\text{O}$ lead to effective collision numbers of 53–670 per molecule per pulse, during which time 3–10 IR photons are absorbed. It is probable from this, and consistent with UV absorption during the IR pulse,^{7b} that collisional relaxation toward an equilibrium distribution is not lagging far behind IR absorption in the $\text{C}_5\text{H}_8\text{O}$ experiments.

Partial Averaging. As is well-known, absorption cross sections vary markedly for different microscopic subspecies of the absorbing species. Neglecting interaction of vibration and rotation: for a given vibrational subspecies, $\sigma \approx 0$ for the majority of its rotational subspecies; and for a given rotational subspecies, σ varies specifically with the amount and distribution of vibrational energy, because of the specificity of anharmonic frequency shifts.^{6,18a} Thus, when it turns out that σ^{exptl} is insensitive to changes in the overall molecular energy distribution, one must infer the existence of mechanisms for partial, but nonetheless effective, microscopic averaging.

Medium-sized and large molecules have certain properties that distinguish them from smaller molecules and which may be relevant toward simplifying their IR absorption laws.

(1) At and above room temperature, the heat capacity for vibration (V) is much greater than that for translation and rotation (T/R), so that $V - T/R$ relaxation during the laser pulse (whose rate varies with P) will not drastically change the vibrational energy.

(2) The rotational fine structure of vibrational bands is very dense, so that homogeneous broadening (i.e., lifetime broadening) of the fine-structure components will have no effect on the overall cross section in the absence of IR saturation^{18b,c}—although it will reduce saturation.^{18c}

(3) At room temperature and above, the density of vibrational states [$g(E_v)$] is high, at vibrational energies attained by most molecules. For C_6F_6 , when E_v equals the mean vibrational energy at 298 K, $g(E_v)$ equals 57 states/wavenumber. After absorption by such molecules of 2, 4, 8, and 25 (1023 cm^{-1}) photons, $g(E_v)$ becomes 7.6×10^4 , 1.4×10^7 , 3.1×10^{10} , and 6.1×10^{18} . These estimates are based on normal mode frequencies¹⁹ treated by Haarhoff's method²⁰ and are in good agreement with estimates by Whitten and Rabinovitch's method.²¹

Because of the high density of vibrational states at energies attained by most molecules, it is possible to visualize a partial averaging process on the basis of E_v . For definiteness, we shall consider partial averaging of the absorption cross section.

Consider a narrow energy range from E_v to $E_v + \delta E_v$. The size of δE_v is arbitrary, but it must be in the range $g(E_v)^{-1} \ll \delta E_v \ll kT$. The upper limit is chosen so that at statistical equilibrium, the states in the range all have equal populations. The lower limit is chosen so that the number of states, $g(E_v)\delta E_v$, is large enough to yield a representative average $\bar{\sigma}(E_v)$ of their cross sections. The

(16) Garcia, D. Ph.D. Thesis, Brandeis University, 1980, may be consulted for details.

(17) Ireton, R. C.; Ko, A. N.; Rabinovitch, B. S. *J. Phys. Chem.* **1974**, *78*, 1984.

(18) (a) Herzberg, G. "Infrared and Raman Spectra of Polyatomic Molecules"; Van Nostrand: New York, 1945. (b) Kauzmann, W. "Quantum Chemistry"; Academic Press: New York, 1957; pp 578–581. (c) Allen, L.; Eberly, J. H. "Optical Resonance and Two-Level Atoms"; Wiley-Interscience, New York, 1975.

(19) Green, J. H. S.; Harrison, D. J. *J. Chem. Thermodyn.* **1976**, *8*, 529.

(20) Haarhoff, P. C. *Mol. Phys.* **1963**, *7*, 101.

(21) Whitten, G. Z.; Rabinovitch, B. S. *J. Chem. Phys.* **1963**, *38*, 2466. See especially the footnote to Table III.

value of δE_v at which this condition is satisfied will probably depend on E_v ; a plausible guess is that $\delta E_v \approx s/g(E_v)$, where s denotes the number of vibrational modes of the substrate molecule.

It follows from this definition that $\bar{\sigma}(E_v)$ is a smoothly varying equilibrium property of the macroscopic system. However, because the averaging process leading to $\bar{\sigma}(E_v)$ requires only that statistical equilibrium exists within a narrow energy range δE_v including E_v , $\bar{\sigma}(E_v)$ will also characterize nonequilibrium systems whenever the latter condition is satisfied.

A mechanism leading to statistical equilibrium within narrow energy ranges exists. When vibrational state densities are high enough, vibrational relaxation can proceed not only by collisional but also by unimolecular, i.e., intramolecular, processes.^{22,23} At high vibrational energies, unimolecular relaxation can be very fast, with picosecond time scales.^{22,23} It occurs with conservation of energy (interpretable, for microscopic processes, in terms of the Uncertainty Principle) and thus can establish statistical equilibrium only within quite narrow energy ranges. But at high vibrational state densities, the partial averaging achieved at the given E_v in an overall nonequilibrium system may be quite effective.

It is desirable to adopt a characteristic name for this unimolecular process of vibrational relaxation. J. W. Gibbs in his writings used the term "isodynamic" for processes taking place at constant energy. We shall accordingly use the term *isodynamic relaxation* and, when the process is fast enough, shall refer to the resulting steady state as a state of *isodynamic equilibrium*.²⁴

Mean-Value Approximation. We now wish to show that the existence of isodynamic equilibrium implies that the phenomenological cross section $\bar{\sigma}(t_1)$ at any time t_1 is virtually independent of the shape of the molecular energy distribution. To simplify notation and follow precedent,⁵ we shall henceforth express E_v as a multiple (n) of the IR photon energy $N_0 h \nu$, as in (9). Let

$$E_v = n N_0 h \nu \quad (9)$$

$P(n)$ denote the normalized distribution function for vibrational energy at t_1 . The mean vibrational excitation number \bar{n} for the ensemble is then given by (10) at t_1 . Assume that isodynamic

$$\bar{n} = \int_0^\infty n P(n) dn \quad (10)$$

equilibrium exists throughout the energy range in which $P(n)$ is significant, but make no other assumption concerning the shape of $P(n)$. In particular, $P(n)$ need not be the Boltzmann distribution. However, because of the existence of isodynamic equilibrium, the previously defined equilibrium function $\bar{\sigma}(n)$ [i.e., $\bar{\sigma}(E_v)$] will characterize any $P(n)$. On this basis, $\bar{\sigma}(t_1)$ is given by (11) at t_1 .

$$\bar{\sigma}(t_1) = \int_0^\infty \bar{\sigma}(n) P(n) dn \quad (11)$$

We now wish to show that $\bar{\sigma}(t_1)$ is practically independent of the shape of $P(n)$. Expand $\bar{\sigma}(n)$ in the Taylor series about \bar{n} .

$$\bar{\sigma}(n) = \bar{\sigma}(\bar{n}) + \left(\frac{d\bar{\sigma}}{dn} \right)_{\bar{n}} (n - \bar{n}) + \frac{1}{2} \left(\frac{d^2\bar{\sigma}}{dn^2} \right)_{\bar{n}} (n - \bar{n})^2 + \dots$$

Multiply each term by $P(n)$ and integrate. Note that $\int_0^\infty P(n) dn = 1$, $\int_0^\infty P(n)(n - \bar{n}) dn = 0$, and $\int_0^\infty P(n)(n - \bar{n})^2 dn = s_n^2$, the variance (squared standard deviation) of n . The result is therefore simply (12) at t_1 . Note that while $\bar{\sigma}(t_1)$ is the average

$$\begin{aligned} \bar{\sigma}(t_1) &= \int_0^\infty P(n) \bar{\sigma}(n) dn \\ &= \bar{\sigma}(\bar{n}) + \frac{1}{2} \left(\frac{d^2\bar{\sigma}}{dn^2} \right)_{\bar{n}} s_n^2 + \dots \end{aligned} \quad (12)$$

cross section for the full ensemble, $\bar{\sigma}(\bar{n})$ is simply the partial average for those molecules whose energy lies in a narrow range centered on $\bar{n}(t_1)$.

In considering the relative magnitudes of terms in (12), we note that $\bar{\sigma}(n)$ is a slowly varying smooth function whose second derivative is necessarily quite small. s_n^2 is of the order of \bar{n} and thus is not very large. As a result, the term involving $d^2\bar{\sigma}/dn^2$ will be small compared to $\bar{\sigma}(\bar{n})$. Higher order terms, not shown explicitly in (12), will be still smaller. In practice, (12) therefore reduces simply to (13) at t_1 . Thus, when isodynamic equilibrium exists,

$$\bar{\sigma}(t_1) \approx \bar{\sigma}(\bar{n}) \quad (13)$$

$\bar{\sigma}(t_1)$ depends in good approximation only on $\bar{n}(t_1)$ and is independent of the shape of the instantaneous distribution $P(n)$.

We shall refer to (13) as the *mean-value approximation*. Analogous approximations may be made for other slowly varying smooth functions of n .

IR Saturation. The apparent absence of IR saturation in the present experiments can also be reconciled with properties normally associated with medium-sized and large molecules. A brief summary will suffice.

For vibrational absorption bands whose rotational fine structure is a dense quasi-continuum, the instantaneous cross section $\bar{\sigma}(I)$ is related to $\bar{\sigma}_0$ according to (14).²⁵ Here m is a dimensionless

$$\bar{\sigma}(I) = \bar{\sigma}_0 / (1 + m \bar{\sigma}_{v,v} I T_1 T_2 / h)^{1/2} \quad (14)$$

parameter of order unity ($2/3 \leq m \leq 2$), $\bar{\sigma}_{v,v}$ is the intrinsic cross section for the vibrational transition obtained from the integrated band intensity (eq 15),²⁶ and T_1 and T_2 are the familiar relaxation

$$N_0 \bar{\sigma}_{v,v} = (\nu_{v,v})^{-1} \int_{\nu,v} \text{band } k(\nu) d\nu \quad (15)$$

times in the optical Bloch equations.^{18c} T_1 and T_2 are shorter than the isodynamic relaxation time. Thus, when isodynamic relaxation is fast, T_1 and T_2 are very short. The denominator in (14), which is the formal analog of a saturation factor, then departs substantially from unity only at rather high intensities. In the present experiments with C_6F_6 , $I_p < 2 \times 10^6$ W cm⁻² throughout. The peak pulse intensity is of course higher, but the instantaneous intensity rarely exceeds 5×10^6 W cm⁻²; $\bar{\sigma}_{v,v} = 6.6 \times 10^{-20}$ cm²/molecule,²⁷ and $m \approx 1$. Thus $[(\bar{\sigma}(I) - \bar{\sigma}_0)/\bar{\sigma}_0] < 0.1$ if $T_1 \approx T_2 < 2 \times 10^{-11}$ s. Except for the reservation stated below, this is an acceptable value for isodynamic relaxation at high vibrational state densities.²²

The preceding calculation is conservative because it neglects the rapid fluctuations in anharmonic frequency shifts associated with isodynamic relaxation, which tend to increase the effective fraction of absorbing molecules and to reduce the effective intensity sensed by such molecules.

Returning to the magnitude of T_1 : an independent method for probing vibrational energy relaxation in polyatomic molecules is through the effects it produces on electronic absorption bands. A recent letter from this laboratory¹⁴ has reported preliminary results for C_6F_6 . IR absorption here was attended by marked changes in UV optical density below 300 nm, and these changes appeared with lag times of 50–110 ns after IR absorption. The lag times were at the margin of measurability with the equipment used, and their significance, though respectable and considerable, is at a lower level than that of the present experiments. If the UV lag times are indeed real, consistency with the present estimates of T_1 can be achieved if it is assumed that UV absorption, in contrast to IR absorption, is sensitive to the shape of $P(n)$, so that the mean-value approximation (eq 13) is poor for UV absorption.

Rate Law. The basis equation is (2). On dissecting E_a into vibrational and T/R energy terms and applying (9) and (10), we obtain (16) for nonlinear molecules. T is the instantaneous T/R

(22) McDonald, J. D. *Annu. Rev. Phys. Chem.* **1979**, *30*, 29.

(23) Oref, I.; Rabinovitch, B. S. *Acc. Chem. Res.* **1979**, *12*, 166.

(24) Gibbs, J. W. "Collected Works"; Longmans, Green and Co.: New York, 1931; Vol. 1, p 3. Gibbs, J. W. *Trans. Conn. Acad. Arts Sci.* **1873**, *2*, 309. The term *isodynamic* seems apt in the present context because much of our knowledge comes from classical molecular trajectory calculation.

(25) Grunwald, E., unpublished research.

(26) Crawford, B., Jr. *J. Chem. Phys.* **1958**, *29*, 1042.

(27) Fujiyama, T.; Crawford, B., Jr. *J. Phys. Chem.* **1968**, *72*, 2174.

$$I^{-1} \frac{dE_a}{dt} = \frac{N_0 h \nu}{I} \frac{d\bar{n}}{dt} + \frac{3R}{I} \frac{dT}{dt} = N_0 \bar{\sigma}(t) \quad (16)$$

temperature and \bar{n} the instantaneous mean excitation number. Simplification results if (17a) $V - T/R$ relaxation is so fast that T is the equilibrium temperature $T(\bar{n})$, or if (17b) $dE_a/dt \gg 3RdT/dt$ and in addition (13) applies.

$$\frac{N_0 h \nu}{I} \frac{d\bar{n}}{dt} + \frac{3R}{I} \frac{dT(\bar{n})}{dt} = N_0 \bar{\sigma}(\bar{n}) \quad (17a)$$

$$\frac{h \nu}{I} \frac{d\bar{n}}{dt} = \bar{\sigma}(\bar{n}) \quad (17b)$$

In order to integrate (17) one needs explicit expressions for $\bar{\sigma}(n)$. As pointed out, for example, by Starov et al.,⁵ $\bar{\sigma}(n)$ is a net cross section, being equal to the difference between cross sections for absorption [$\bar{\sigma}^a(n)$] and induced emission [$\bar{\sigma}^e(n-1)$]. The latter cross sections are introduced so that $\bar{\sigma}(n)$ may be factored into two independent functions of n , as in (18).⁵ $g(n)$ and $g(n-1)$

$$\begin{aligned} \bar{\sigma}(n) &= \bar{\sigma}^a(n) - \bar{\sigma}^e(n-1) \\ &= \bar{\sigma}^a(n) [1 - g(n-1)/g(n)] \end{aligned} \quad (18)$$

denote the vibrational state densities when $E_v = nh\nu$ and $(n-1)h\nu$, respectively. By definition, when $n < 0$, $g(n) = 0$; hence $\bar{\sigma}(0) = \bar{\sigma}^a(0)$.

In the present work, $g(n-1)/g(n)$ was calculated by the method of Haarhoff²⁰ and results fitted to (19), as suggested by Barker.²⁸

$$g(n-1)/g(n) = \alpha n / (1 + \alpha n) \quad (19)$$

The fit of (19) to the state-density ratios was not exact but quite adequate for the present purpose. Values adopted for α were 1/30 for C_6F_6 and 1/32 for C_5H_8O . According to simple theory, α^{-1} should be close to the number of vibrational modes.²⁸

Following Grant et al.,²⁹ $\bar{\sigma}^a(n)$ is sometimes represented as an exponential function $\bar{\sigma}^a(n) = \bar{\sigma}(0) \exp(-bn)$, where b is an experimentally derived parameter. The fit to experimental cross sections is quite good,⁵ although the exponential dependence may underestimate $\bar{\sigma}^a$ at high n . When $b > 0$ we prefer to use the alternative relation (20), which fits about as well and is more convenient to apply. The parameter β in (20) $\approx b$.

$$\bar{\sigma}^a(n) = \bar{\sigma}(0) / (1 + \beta n) \quad (20)$$

On introducing (18), (19), and (20) into (17b) and doing some algebra, we obtain (21). As before, $dF = I dt$ and \bar{n} is the mean

$$h \nu \frac{d\bar{n}}{dF} = \frac{\bar{\sigma}(0)(1 - \delta)}{(1 + \alpha \bar{n})(1 + \beta \bar{n})} \quad (21a)$$

$$\delta = \alpha \beta \bar{n} / (1 + \beta \bar{n}) < \alpha \quad (21b)$$

excitation number of the molecular system at time t . For medium-sized and large molecules, $\alpha \ll 1$; hence $1 - \delta \approx 1$. Separation of variables and integration over the full IR pulse then leads to (22). In the above, \bar{n}_0 and \bar{n}_f denote \bar{n} at beginning and

$$\frac{\bar{\sigma}(0)}{h \nu} \int_0^{F_p} dF = \int_{\bar{n}_0}^{\bar{n}_f} d\bar{n} (1 + \alpha \bar{n})(1 + \beta \bar{n}) \quad (22a)$$

$$\begin{aligned} \frac{\bar{\sigma}(0)}{h \nu} F_p = \\ (\bar{n}_f - \bar{n}_0) [1 + (\alpha + \beta)(\bar{n}_f + \bar{n}_0)/2 + \alpha \beta (\bar{n}_f^2 + \bar{n}_f \bar{n}_0 + \bar{n}_0^2)/3] \end{aligned} \quad (22b)$$

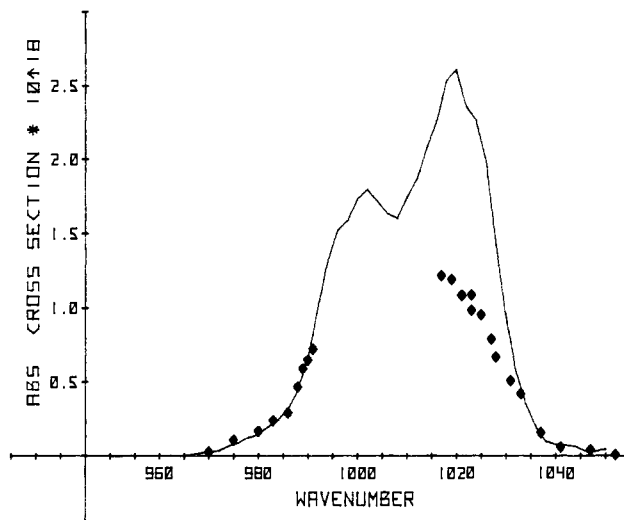


Figure 4. Absorption cross section vs. wavenumber for the 1000- and 1020-cm⁻¹ absorption band of C₆F₆: solid curve, results by low-intensity spectrophotometry; diamonds, σ^{exptl} based on laser irradiation at a fluence of 0.15 J cm⁻².

end of the IR pulse, respectively. When (17b) applies, $\bar{n}_f - \bar{n}_0 = E_{\text{abs}}/(N_0 h \nu)$. Substituting in (1), one then obtains (23).

$$\begin{aligned} \sigma^{\text{exptl}} = \\ \bar{\sigma}(0) / [1 + (\alpha + \beta)(\bar{n}_f + \bar{n}_0)/2 + \alpha \beta (\bar{n}_f^2 + \bar{n}_f \bar{n}_0 + \bar{n}_0^2)/3] \end{aligned} \quad (23)$$

When $V - T/R$ relaxation can not be neglected, an appropriate alternate calculation must be made to relate E_{abs} to \bar{n}_0 and \bar{n}_f and thus arrive at a model equation for σ^{exptl} . The preceding treatment (22) and/or (23) assumes that the absorbing mode is nondegenerate.

Parameters of the Rate Law. For 2,3-dihydropyran the mode of IR excitation is the nondegenerate C-O stretch centered at 1074 cm⁻¹. Excitation at 1072 cm⁻¹ takes place in the flat portion of the absorption band near the maximum. Since the time for relaxation to thermal equilibrium in the given pressure range is known to be only a small fraction of the SPE pulse width,^{7b} in fitting the data for $E_{\text{abs}}/(N_0 F)$ to (22), values used for \bar{n}_f assume full $V - T/R$ relaxation and are typically 10–20% smaller than $\bar{n}_0 + E_{\text{abs}}/(N_0 h \nu)$.

The $\bar{\sigma}(0)$ parameter for the present data (Figure 3) is 0.413×10^{-18} cm², in good agreement with $\bar{\sigma}_0 = 0.423 \times 10^{-18}$ cm² obtained by IR spectrophotometry. β is 0.115. This is a relatively large value (cf. ref 5) and implies, for instance, that at 1000 K $\sigma^{\text{exptl}}/\bar{\sigma}(0)$ is only 0.60.

For hexafluorobenzene the mode of IR excitation is the degenerate ring deformation (ν_{13} , symmetry species e_{1u})^{19,30} with band maximum at 1020 cm⁻¹. The $\nu = 1$ state of this mode is believed to be in Fermi resonance with a combination state of E_{1u} symmetry located ~ 1000 cm⁻¹ above the ground state, for which various reasonable descriptions have been given.^{19,30} The experiments reported in Figure 1 and 2 were done at 1023 cm⁻¹. But before analyzing them, it is instructive to consider similar data obtained for a range of wavenumbers.

Figure 4 shows low-intensity cross sections ($\bar{\sigma}_0$) measured by IR spectrophotometry and comparable values of σ^{exptl} measured at a constant fluence of 0.15 J/cm². (CO₂ laser lines R12–R48 of 00°1–10°0 and P50–P14 of 00°1–02°0 were used.) Relatively far from 1020 cm⁻¹, σ^{exptl} and $\bar{\sigma}_0$ are seen to be in good agreement. The two functions diverge as 1020 cm⁻¹ is approached, however, and $\sigma^{\text{exptl}}/\bar{\sigma}_0$ reaches about 0.5 at 1020 cm⁻¹.

Because of the fairly good agreement between $\bar{\sigma}_0$ and low-fluence σ^{exptl} obtained in other cases,^{5,31} the present pattern seems

(28) Barker, R. J. *J. Chem. Phys.* **1980**, *72*, 3686.

(29) Grant, E. R.; Schulz, P. A.; Sudbo, A. S.; Shen, Y. R.; Lee, Y. T. *Phys. Rev. Lett.* **1978**, *40*, 115.

(30) Eaton, V. J.; Pearce, R. A. R.; Steele, D.; Tindle, J. W. *Spectrochim. Acta, Part A* **1976**, *32A*, 663 and references cited therein.

intriguing and significant, but we must leave its analysis to others who may be more expert in this matter. The ν_{13} mode is twofold degenerate and, since $\sigma^{\text{exptl}}/\bar{\sigma}_0$ approaches ~ 0.5 , one is tempted to speculate that twofold degeneracy is somehow removed by the IR laser field even at the lowest fluence used.

Be that as it may, the data in Figure 1, at 1023 cm^{-1} , seem well-behaved in terms of eq 23 (whose use implies that $V-T/R$ relaxation may be neglected). $\bar{\sigma}(0) = 1.45 \times 10^{-18} \text{ cm}^2$ compared with $\bar{\sigma}_0 = 2.3 \times 10^{-18} \text{ cm}^2$. $\beta = 0.023$.

(31) The equation for the rate of absorption from a coherent source in the steady state is the same as that for absorption from a chaotic source. Compare ref 6 with eq 3-67 of: Pople, J. A.; Schneider, W. G.; Bernstein, H. J. "High Resolution Nuclear Magnetic Resonance"; McGraw-Hill: New York, 1959 and rewrite the latter in terms of variables for optical resonance. A factor of 0.5, derived just preceding eq 3-67, was erroneously omitted from (3-67).

If the mode degeneracy is included, rate law 21a changes to (24), to the same order of approximation. The integrated form

$$h\nu \frac{d\bar{n}}{dF} = \frac{\bar{\sigma}(0)}{(1 + \alpha\bar{n})^2(1 + \beta\bar{n})} \quad (24)$$

of (24) was found to reproduce the data for C_6F_6 about as well as did eq 23—5.8% vs. 5.9% for the standard error of fit. $\bar{\sigma}(0)$ is $1.46 \times 10^{-18} \text{ cm}^2$, about the same as before. β is -0.007 , with a standard error of ~ 0.01 . Thus the data permit the interpretation that $\bar{\sigma}^a$ is constant.

Concluding Remarks. It has been argued that the relatively simple absorption laws observed particularly for C_6F_6 are related to physical properties generally shared by medium-sized and large molecules and thus are not limited to the present substrates. Further work toward testing this hypothesis is in progress.

Photochemical Transformations. 30. Photosolvolytic of Benzyl Chlorides in *tert*-Butyl Alcohol. 2. Nature of Excited States[†]

Stanley J. Cristol* and Thomas H. Bindel

Contribution from the Department of Chemistry, University of Colorado, Boulder, Colorado 80309. Received November 13, 1980. Revised Manuscript Received August 18, 1981

Abstract: The photosolvolytic of a number of benzyl chlorides in *tert*-butyl alcohol, both as a result of direct irradiation and ketone triplet sensitization, has been studied. A variety of sensitization and quenching techniques have been used. The results obtained are rationalized by the assumption that there are two triplet states of the benzyl chlorides accessible in these experiments—one a short-lived upper state, which leads to solvolysis product, and another a long-lived (lower energy) state, which reverts to ground-state reactant. Consistent with this idea, *m*-methoxybenzyl chloride is shown to quench the photoreactions of benzophenone with benzhydrol without the formation of a significant amount of reactive species. The effects of wavelength on the reactions of *p*-acetobenzyl chloride are measured and discussed in terms of the two-triplet concept.

Recently, several research groups have reported their studies on the photochemistry of benzyl chloride in nucleophilic solvents.²⁻⁷ Much of the literature deals with the effects of photosensitization, of direct irradiation, and of solvent changes upon quantum yields of photoinduced bond heterolysis and homolysis for benzyl chloride itself, although we⁶ have recently reported results with a variety of substituted benzyl chlorides for reactions in *tert*-butyl alcohol. In general, direct irradiation has been reported to lead to lower quantum yields for heterolytic (photosolvolytic) products than does photosensitization, while the opposite is true for the homolytic (radical) products. Several problems remained and seemed reasonable for us to attack. Among these is the question of whether the intermediates leading to photosolvolytic products were identical, whether produced by sensitization (direct formation of triplet state) or by direct irradiation (singlet formation, possibly followed by intersystem crossing to triplet). Further questions include whether the excited-state intermediates of a given multiplicity leading to photosolvolytic are the same as those leading to homolysis, that is, where does branching occur in the photo-reaction scheme? With a variety of substituted benzyl chlorides available, one might be able to measure the effect of structure upon reactivity, both in the sense of excitation-transfer rates from sensitizer to substrate and in the sense of excited substrate decay to product-forming intermediate. Finally, a problem of general concern in photochemistry is the question of energy wastage. This paper describes initial work in our attempt to address several of these problems.

[†] Dedicated to George S. Hammond on the occasion of his 60th birthday.

Methods and Results

There are a variety of methods available for learning about the excited-state intermediates in photochemical reactions, although the limitations of each are often overlooked. Of these, fluorescence spectroscopy and fluorescence decay rates or phosphorescence spectroscopy and phosphorescence decay rates are very useful,⁸ but require the assumption that the species whose emission is measured is the product-determining intermediate. With greater time resolution spectroscopy, it is often possible to see more than one excited-state species by such means, but again the assignment of emissions to intermediates remains difficult, as does the quenching of fluorescence or of phosphorescence in the Stern-Volmer method.⁹

(1) Paper 29: Cristol, S. J.; Optiz, R. J.; Bindel, T. H.; Dickenson, W. A. *J. Am. Chem. Soc.* **1980**, *102*, 7977.

(2) Ivanov, V. B.; Ivanov, V. L.; Kuz'min, M. G. *J. Org. Chem. USSR (Engl. Transl.)* **1973**, *9*, 345.

(3) Cristol, S. J.; Greenwald, B. E. *Tetrahedron Lett.* **1976**, 2105.

(4) Hyömäki, J.; Koskikallio, J. *Acta Chem. Scand., Ser. A* **1977**, *A31*, 321.

(5) (a) Brocklehurst, B.; Appleton, D. C.; McKenna, J.; McKenna, J. M.; Smith, M. J.; Taylor, P. S.; Thackeray, S.; Walley, A. R. *J. Chem. Soc., Chem. Commun.* **1977**, 108. (b) *J. Chem. Soc., Perkin Trans. 2* **1980**, 87.

(6) Cristol, S. J.; Bindel, T. H. *J. Org. Chem.* **1980**, *45*, 951.

(7) Larson, J. R.; Epiotis, N. D.; McMurchie, L. E.; Shaik, S. S. *J. Org. Chem.* **1980**, *45*, 1388.

(8) Turro, N. J. "Modern Molecular Photochemistry"; Benjamin/Cummings: Menlo Park, Calif., 1978; Chapter 5.

(9) Stern, O.; Volmer, M. *Phys. Z.* **1919**, *20*, 183.